

Control of vortex shedding in a two-dimensional flow past a plate

R. Shermer*

Physics Department, Center for Complex Systems Research, Beckman Institute, University of Illinois, Urbana, Illinois 61801
(Received 14 February 1992)

A version of the no-feedback-control method developed by Hübler and Lüscher [Helv. Phys. Acta **62**, 544 (1989)] is applied to two-dimensional open-channel flow past a plate. The control is applied in the vortex-shedding regime with the aim of reducing the effective Reynolds number, thereby suppressing the vortex shedding. It is shown that the method works well not only when the flow is globally forced but also when the forcing is restricted to the boundary-layer region.

PACS number(s): 47.90.+a, 02.70.+d, 47.10.+g

I. INTRODUCTION

The quest for successful control of hydrodynamic systems is one of the most exciting challenges in the fluid and control sciences today. Developing a systematic method for controlling fluid systems effectively will allow new technologies to emerge and could make older ones more efficient.

Much work has been conducted recently into altering fluid behavior via external forcing [1–14]. There are various approaches taken to the idea. In the open-loop approach, the experimenter makes measurements on the system, Fourier analyzes the data to determine the primary frequencies, and then adjusts the frequency of the driving force based on that analysis. The driving force in the majority of cases is sinusoidal with one or two frequencies. Feedback control methods have also been applied to fluid experiments. In most cases, the forcing has been limited to sinusoidal oscillations in time with little or no spatial complexity.

An alternative approach to spatial control known as model-based control [15] allows the determination of a driving force of the appropriate complexity. In fact, the driving force is determined so that the desired asymptotic behavior is a solution to the forced system. The idea is to use a model to predict what the system will do and then use the information from this complete description of the flow field, rather than from limited measurements, to compute the control force. Using a model to predict the behavior of the system means that calculations for the control need not take place in real time. Furthermore, no complicated measurements or real-time signal processing is necessary.

The paper is arranged as follows. In the theory section, the general approach of the method is described as it applies to systems governed by partial differential equations. The driving force is then computed for general Navier-Stokes problems in the common formulations. The stability issues are also addressed. Details of the numerical simulations are described at the beginning of the results section. A simple numerical experiment involving open-channel flow with a plate is the main focus. In the first part of the study the driving force is applied

to each grid point at each time step, as specified by the original development of the method. In the second part of the tests, the driving force is restricted to a localized region; applied only to a neighborhood of points around the plate. Some further discussions and directions are given in the summary.

II. THEORY

The ideas presented here are extensions of the control technique developed by Hübler and Lüscher [16]. Various directions have since been explored [17–21]. A detailed study of model-based control applied to a restricted class of ordinary differential equations was recently published by Jackson [22]. Work by Jackson and Hübler [23] and Jackson [24] explores the criteria needed for successful application of this theory for maps. Some progress has been reported in the realm of partial differential equations [15, 25]. The present work focuses primarily on the application of the spatial theory to hydrodynamic systems.

Model-based control works by determining the correct driving force to make the goal dynamics a solution to the forced experiment. For any spatially extended system, we define the *experiment* as a state vector field, $\mathbf{u}(\mathbf{x}, t)$, $\mathbf{x} \in \mathbb{R}^n$ and the dynamical equations of motion,

$$\dot{\mathbf{u}}(\mathbf{x}, t) = \mathbf{E}(\mathbf{u}, \mathbf{x}, t) + \mathbf{f}(\mathbf{x}, t) \quad (1)$$

that govern the time evolution of the field. Unlike standard feedback controls, a *goal* dynamics must be explicitly chosen:

$$\dot{\mathbf{w}}(\mathbf{x}, t) = \mathbf{G}(\mathbf{w}, \mathbf{x}, t). \quad (2)$$

Since our knowledge of the experiment is not exactly the experiment itself, an intermediate set of equations known as the *model* is often defined for the purpose of investigating the behavior of the control in the presence of model errors,

$$\dot{\mathbf{v}}(\mathbf{x}, t) = \mathbf{M}(\mathbf{v}, \mathbf{x}, t). \quad (3)$$

After substitution of the goal field into the experiment

equation, replacing the experiment dynamics with the model, and solving for the force, we find the equation for the force,

$$\mathbf{F}(\mathbf{x}, t) = \mathbf{G}(\mathbf{w}, \mathbf{x}, t) - \mathbf{M}(\mathbf{w}, \mathbf{x}, t). \quad (4)$$

This equation gives the correct form of the forcing so that $\mathbf{w}(\mathbf{x}, t)$ is a solution to the driven experiment, Eq. (1) when the model is exact.

The boundary conditions in (2) used to determine $\mathbf{F}(\mathbf{x}, t)$ should be the same as those in (1), since the driving force does not account for any possible differences. Given both systems with fixed but different boundary conditions, a boundary layer will form where there will be no entrainment. The size and behavior of this region is dependent on the nature of the equations and the difference in the specified boundary conditions. If the aim of the control is to change the value of the experiment at the boundary, an additional driving force must be applied to that region.

For identical initial and boundary conditions, and $\mathbf{M} = \mathbf{E}$, the experiment immediately entrains to the goal dynamics. Granted, this is not sufficient to guarantee success in an actual application. It must further be shown that the solution is stable under perturbations of noise and differences in both the initial and the boundary conditions.

Limited stability analysis has been worked out for a few partial differential equations [15, 25]. The only technique that has yielded useful information at this point has been determined by defining a difference dynamics, $\epsilon = u - w$, governed by

$$\dot{\epsilon} = E(\epsilon + w, \mathbf{x}, t) - M(w, \mathbf{x}, t). \quad (5)$$

The boundary conditions for this problem are computed as the differences (errors) between the experiment and the goal boundary conditions. The initial conditions are obtained in the same manner.

The control technique can be written down for the Navier-Stokes equations in each of the standard formulations. For the stream-vorticity form,

$$\dot{\omega} = -\frac{\partial\psi}{\partial y}\frac{\partial\omega}{\partial x} + \frac{\partial\psi}{\partial x}\frac{\partial\omega}{\partial y} + \mu\nabla^2\omega + \mathbf{F}(\mathbf{x}, t), \quad (6)$$

$$\nabla^2\psi + \omega = 0, \quad (7)$$

and a goal dynamics that is identical in form but with a larger viscosity, the driving force is

$$\mathbf{F}(\mathbf{x}, t) = (\mu' - \mu)\nabla^2\varpi. \quad (8)$$

ϖ is the corresponding goal variable for ω .

For the incompressible form and a goal dynamics of a higher viscosity, the force is similarly,

$$\dot{\mathbf{u}} = -(\mathbf{u} \cdot \nabla)\mathbf{u} - \nabla P + \mu\nabla^2\mathbf{u} + \mathbf{F}(\mathbf{x}, t), \quad (9)$$

$$\nabla \cdot \mathbf{u} = 0, \quad (10)$$

$$\mathbf{F}(\mathbf{x}, t) = (\mu' - \mu)\nabla^2\mathbf{w}. \quad (11)$$

The density in the incompressible form and the stream function in the vorticity form are not dynamically specified. That is, neither variable is defined by a time evo-

lution equation. Instead, they are each constrained by Poisson equations. Such variables are often treated as Lagrange multipliers and the equations that specify them, constraints. The lack of dynamic specification implies that there is no straightforward way to define a different goal dynamics for those variables, or compute time dependent driving forces for the equations that define them. Any variable behaving as such should be left alone. This is equivalent to the requirement that the goal dynamics for the variable be specified by the same constraint equation as that of the experiment.

The compressible form of the Navier-Stokes equations,

$$\dot{\mathbf{u}} = -(\mathbf{u} \cdot \nabla)\mathbf{u} - \frac{1}{\rho}\frac{\partial P}{\partial\rho}\nabla\rho + \frac{1}{\rho}\mu\nabla^2\mathbf{u} + \mathbf{F}(\mathbf{x}, t), \quad (12)$$

$$\dot{\rho} = -\nabla \cdot (\rho\mathbf{u}), \quad (13)$$

requires an equation of state,

$$P(\rho) = f(\rho). \quad (14)$$

The driving force is

$$\mathbf{F}(\mathbf{x}, t) = \frac{\mu' - \mu}{\rho'}\nabla^2\mathbf{w}. \quad (15)$$

By adding an additional forcing term to Eq. (13), the density field can also be modified.

With the same equation of state, and goal functions w and σ , the ϵ stability equation is

$$\begin{aligned} \dot{\epsilon} = & -(\epsilon \cdot \nabla)\epsilon - (\mathbf{w} \cdot \nabla)\epsilon - (\epsilon \cdot \nabla)\mathbf{w} \\ & - \frac{\partial P}{\partial\rho}(\rho\nabla\sigma - \sigma\nabla\rho) \\ & + \frac{\mu}{\rho}\nabla^2\epsilon + \left(\frac{\mu}{\rho} - \frac{\nu}{\sigma}\right)\nabla^2\mathbf{w}, \end{aligned} \quad (16)$$

$$\dot{\delta} = -\nabla \cdot (\delta\epsilon + \delta\mathbf{w} + \sigma\epsilon). \quad (17)$$

Solving Eqs. (16) and (17) would determine exactly the necessary conditions for the control to succeed or fail and yield the rate of convergence to the goal flow field from the given initial conditions. The form of these equations is particularly difficult, hence no attempt has been made to solve the equations once they have been written down. The equations are shown to emphasize the difficulty of working with a Navier-Stokes system and to show due justification for exploring the behavior of these systems numerically.

Previous work indicated that model-based control should work under at least some circumstances for the Navier-Stokes equations. Past results indicated that the stability of the control is linked with the dissipative nature of the experiment's equations. Numerical work suggests that if the experiment has dissipation in a region, the control succeeds in that region. Viscous terms seem crucial to the stability while hyperbolic terms appear neutral. It is believed that the pressure term could also help in the stability.

III. RESULTS

Numerical simulations of Eqs. (12)–(15) were conducted to determine the stability of the control directly. The simulation is of an open-channel flow with a vertical plate obstruction. The experiment was run in a vortex shedding range while the goal was chosen to be a laminar flow field.

The computational grid consists of an open-flow channel similar to that of Fromm and Harlow [26]. The channel is 60 grid points from wall to wall and 120 grid points from inlet to outlet. A thin rectangular plate 3 sites long and 10 wide is situated 19 sites from the inlet and centered vertically. The computation was written to simulate the compressible Navier-Stokes equations using a finite difference scheme.

The experiment was chosen to be a flow with an approximate Reynolds number of $Re = 200$. The boundary conditions of both goal and experiment were identical. No noise was added to the experiment—thus the model was exact to within the numerical accuracy of the simulations. The goal equation was chosen to obey the same equations but with a lower Reynolds number. The same equation of state was chosen for both experiment and goal. Additionally, the density of the goal and the experiment were each determined by the standard equation of conservation.

The goal was chosen to be a laminar steady-state flow with approximate Reynolds number, $Re = 20$ in order to reduce the amount of computation necessary. The control driving force could then be computed in the following manner. The goal simulation was turned on from an artificial initial condition and then allowed to settle to a steady laminar flow as shown in Fig. 1. At this point the velocity and pressure fields of the goal for just one time step were stored for future use. The experiment was initiated and allowed to run until all transients had passed and the flow had developed the usual von Karman vortex street as in Fig. 2. Arbitrarily beyond this point, the driving force, shown in Eq. (15), which was computed from the stored goal data, was applied at each time step of the experiment. This time-independent approximation of the driving force is only valid when the goal is chosen

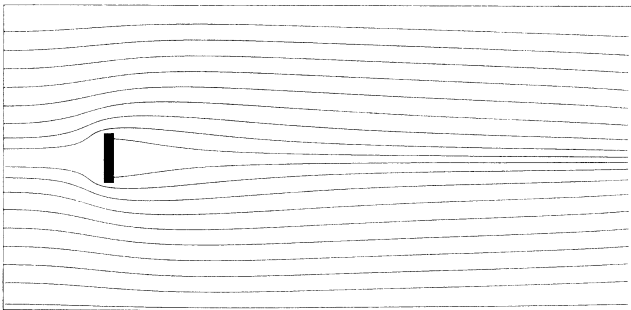


FIG. 1. Velocity profile of the goal after the transients have passed (40 s). Simulation parameters were the same as for Fig. 2 except the viscosity was chosen to be $\mu = 1.0$, yielding an approximate Reynolds number of 20.

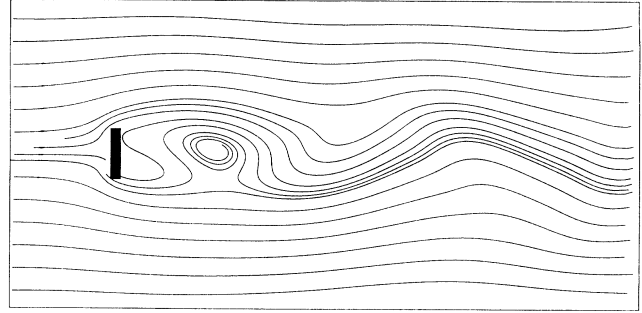


FIG. 2. Velocity profile of the uncontrolled experiment [integration of Eqs. (12)–(14), with $\mathbf{F}(\mathbf{x}, t) = \mathbf{0}$] after the transients have passed ($t > 800.0$ s). The number of computational grid sites is 60 in the vertical direction and 120 in the horizontal. The fluid enters at the left and leaves at the right. The upper and lower boundaries are no-penetration walls of the channel moving at u_∞ . An obstacle in the form of a flat plate is positioned 18 grid points from the inlet. The length of the plate is 10 sites and the width is 3. Simulation parameters were $u_\infty = 0.8$, $p_\infty = 1.0$, $\mu = 0.01$. With the numerical viscosity accounted for, the Reynolds number is approximately $Re = 200$.

to be a steady-state flow field. No information about the present state of the experiment was incorporated into the driving force. The simulation was allowed to settle before producing Fig. 3.

The control worked reasonably well in that the vortex shedding halted after about 500 s. The controlled experiment's flow field shown in Fig. 3 is close but not identical to that of the goal flow field in Fig. 1. There may be several causes for this behavior. The most significant influence is believed to arise from an incorrect estimation of the numerical viscosity inherent to the computational method used.

Using boundary flow fields determined from the previous simulations a second computation was run to test whether favorable control could still be effected when the driving force applied only to a localized region around the

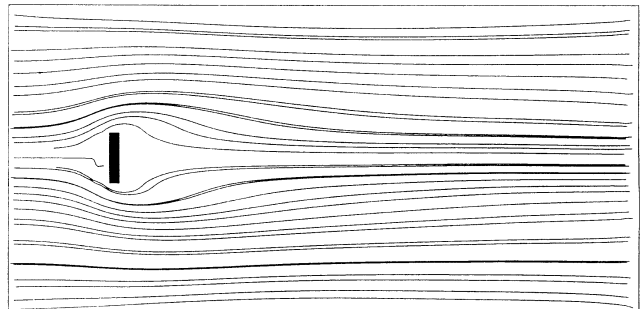


FIG. 3. Velocity profile of the controlled experiment [integration of Eqs. (12)–(14), with an applied force as defined in (15).] Compare the profile with that of both the uncontrolled experiment and the goal. The flow pattern is close to that of the goal but not quite identical. Simulation parameters are the same as for the uncontrolled experiment (Fig. 2), but with the additional body force applied.

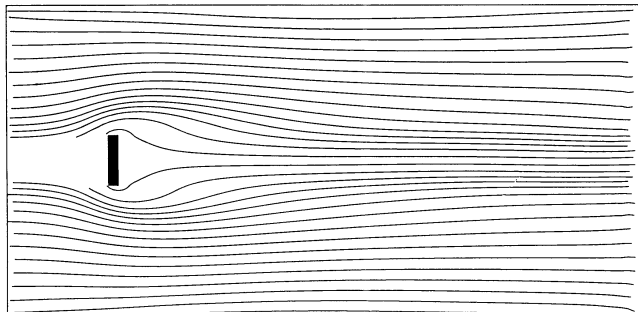


FIG. 4. The control scenario here is the same as in Fig. 3 except that the forcing has been spatially localized to a region around the plate. The flow is not identical to the goal flow in Fig. 1, but it appears to be very close to the flow in Fig. 3, indicating that some model error still exists. The residual model error comes from the error in estimating the numerical viscosity. The force was limited to the region $16 < y < 44$ vertically and $18 < x < 22$ horizontally.

plate. Though this approach may appear intuitively acceptable, it must be stressed that $\mathbf{w}(x, t)$ is now no longer a solution of the forced experiment. $\mathbf{F}(x, t)$ is no longer the correct driving force for the specified $\mathbf{w}(x, t)$.

As before, the experiment was brought to the periodic shedding stage before the control was applied. The control was applied to the boundary layer at each iteration. The system was allowed to run for several thousands of iterations. The results are shown in Fig. 4. The control not only worked well, it worked as well as the globally forced system. The reason being that the force, $\mathbf{F}(x, t) \propto \nabla^2 \mathbf{w}(x, t)$ and $\nabla^2 \mathbf{w}(x, t)$, decays rapidly away from the plate.

IV. SUMMARY

I have attempted to demonstrate the potential usefulness of Hübler's model-based control method in hydrodynamic applications through a simple open-channel flow example.

This control method appears to be stable for systems governed by the Navier-Stokes equations; suggesting a systematic method for developing complex control forces appropriate in hydrodynamic applications. Though the method formally specifies a global body force that cannot be realistically applied in most situations, the potential exists for reducing the scope and dimensionality of the force—possibly limiting it to an airfoil boundary.

A major potential advantage of the method is that the engineer would have complete freedom to choose the goal dynamics. One would not be limited to just driving forces that damp out the characteristic dynamics but may choose from a nearly limitless variety of goals.

Another advantage of the approach is that the calculation yields the full complexity of the driving force rather than just the fundamental frequency in the first-order linear open-loop approach. The method computes the correct nonlinear driving force to essentially all orders being limited only by the spatial and temporal accuracy of the simulations.

ACKNOWLEDGMENTS

The author wishes to thank Alfred Hübler, Paul Newton, Atlee Jackson, and Norman Packard for many timely discussions and helpful suggestions. This work was partially supported by the National Science Foundation, Grant Nos. Phy86-58062 and DMS91-05813, and by the Office of Naval Technology.

* Present address: Magnetics Group Code R43, Naval Surface Warfare Center at White Oak, Silver Spring, MD 20903-5000.

- [1] P. J. Strykowski and K. R. Sreenivasan, *J. Fluid Mech.* **218**, 71 (1990).
- [2] K. J. Olinger and K. R. Sreenivasan, *Phys. Rev. Lett.* **60**, 797 (1988).
- [3] M. Gharib and K. Williams-Stuber, *J. Fluid Mech.* **208**, 225 (1989).
- [4] K. S. Breuer, J. H. Haritonidis, and M. T. Landahl, *Phys. Fluids A* **1**, 574 (1989).
- [5] L. D. Kral and H. F. Fasel, *AIAA J.* **29**, 1407 (1991).
- [6] J. J. Miao, K. C. Lee, M. H. Chen, and J. H. Chou, *AIAA J.* **29**, 1140 (1991).
- [7] E. Roesch, H. Eckelmann, and A. Hübler (unpublished).
- [8] M. Nishioka, M. Asai, and S. Yoshida, *AIAA J.* **28**, 1909 (1990).
- [9] Fei-Bin Hsiao, Chin-Fung Liu, and Jong-Yaw Shyu, *AIAA J.* **28**, 1440 (1990).
- [10] A. Bar-Sever, *AIAA J.* **27**, 820 (1989).
- [11] Mohamed Gad-el-Hak and Ron F. Blackwelder, *AIAA J.* **27**, 308 (1989).
- [12] S. Biringen, W. E. Nutt, and M. J. Caruso, *AIAA J.* **25**, 239 (1987).
- [13] X. Y. Huang, *AIAA J.* **25**, 1126 (1987).
- [14] L. Maestrello and Ting Lu, *AIAA J.* **23**, 1038 (1985).
- [15] R. Shermer, A. Hübler, and N. Packard, *Phys. Rev. A* **43**, 5642 (1991).
- [16] A. Hübler and E. Lüscher, *Helv. Phys. Acta* **62**, 544 (1989).
- [17] A. Hübler and E. Lüscher, *Naturwissenschaften* **76**, 67 (1989).
- [18] A. Hübler, *Helv. Phys. Acta* **62**, 343 (1989).
- [19] T. Meyer, A. Hübler, and N. Packard, in *Measures of Complexity and Chaos*, edited by N. B. Abraham, A. M. Albano, A. Passamante, and P. E. Kapp (Plenum, New York, 1989).
- [20] K. Chang, A. Hübler, and N. Packard, in *Measures of Complexity and Chaos* (Ref. [19]).
- [21] D. Bensen, M. Welge, A. Hübler, and N. Packard, in *Measures of Complexity and Chaos* (Ref. [19]).
- [22] E. A. Jackson, *Phys. Lett. A* **151**, 478 (1990).
- [23] E. A. Jackson and A. Hübler, *Physica D* **44**, 407 (1990).
- [24] E. A. Jackson, *Phys. Rev. A* **44**, 4839 (1991).
- [25] R. Shermer, Ph. D. thesis, University of Illinois at Urbana-Champaign, 1991.
- [26] J. E. Fromm and F.H. Harlow, *Phys. Fluids* **6**, 975 (1963).